Puccinia striiformis f. sp. tritici microRNA-like RNA 1 (Pst-milR1), an important pathogenicity factor of Pst, impairs wheat resistance to Pst by suppressing the wheat pathogenesis-related 2 gene

Bing Wang[1], Yanfei Sun[2], Na Song[2], Mengxin Zhao[2], Rui Liu[2], Hao Feng[2], Xiaojie Wang[2] and Zhensheng Kang[2]

[1]State Key Laboratory of Crop Stress Biology for Arid Areas and College of Life Sciences, Northwest A&F University, Yangling, Shaanxi 712100, China; [2]State Key Laboratory of Crop Stress Biology for Arid Areas and College of Plant Protection, Northwest A&F University, No. 3 Taicheng Road, Yangling, Shaanxi 712100, China

Authors for correspondence:
Zhensheng Kang
Tel: +86 02987080061
Email: kangzs@nwsuaf.edu.cn

Xiaojie Wang
Tel: +86 02987081317
Email: wangxiaojie@nwsuaf.edu.cn

Summary

- Small RNAs (sRNAs), an important type of pathogenicity factor, contribute to impairing host immune responses. However, little is known about sRNAs in *Puccinia striiformis* f. sp. *tritici* (*Pst*), one of the most destructive pathogens of wheat (*Triticum aestivum* L.). Here, we report a novel microRNA-like RNA (milRNA) from *Pst* termed microRNA-like RNA 1 (*Pst*-milR1), which suppresses wheat defenses during wheat–*Pst* interactions.

- We identified *Pst*-milR1 as a novel milRNA in *Pst*. Biological prediction and co-transformation showed that *Pst*-milR1 takes part in cross-kingdom RNA interference (RNAi) events by binding the wheat pathogenesis-related 2 (*PR2*) gene.

- Silencing of the *Pst*-milR1 precursor resulted in increased wheat resistance to the virulent *Pst* isolate CYR31. *PR2* knock-down plants increased the susceptibility of wheat to the avirulent *Pst* isolate CYR23. This suggests that *Pst*-milR1 represses the plant immune response by suppressing the expression of *PR2*.

- Taking our findings together, we postulate that *Pst*-milR1 is an important pathogenicity factor in *Pst*, which acts as an effector to suppress host immunity. Our results provide significant new insights into the pathogenicity of the stripe rust pathogen.

Introduction

RNA interference (RNAi) is a conserved eukaryotic mechanism in which small RNAs (sRNAs) are involved in the maintenance of RNA stability, RNA processing, biotic stress responses, and the regulation of morphological and developmental processes (Dang *et al.*, 2011). sRNAs are produced from hairpin-structured or double-stranded RNA (dsRNA) by RNase III-like endonucleases called Dicers (Bartel, 2004). The silencing effects mediated by sRNAs in different pathways require an Argonaute/Piwi protein as the core component of the RNA-induced silencing complex (RISC; Ghildiyal & Zamore, 2009; Kim *et al.*, 2009). A number of sRNA classes have been described in plants and animals. Based on whether their biogenesis is dependent on Dicer, the known eukaryotic sRNAs can be classified as Dicer-dependent or Dicer-independent (Lee *et al.*, 2010). The Dicer-dependent group of sRNAs includes various small interfering RNAs (siRNAs) and microRNAs (miRNAs; Ghildiyal & Zamore, 2009).

miRNAs are a class of negative post-transcriptional regulators of gene expression. Mature miRNAs consist of 20–24 nucleotides, which are processed from single-stranded primary miRNA with unique stem-loop structures (Bartel, 2004). miRNAs negatively regulate gene expression by binding to the open reading frame or untranslated regions (UTRs) of specific target genes (Lau *et al.*, 2013). Moreover, miRNAs also play key roles in differentiation, carcinogenesis, and immunoreaction in animals (Croce, 2009; Xiao & Rajewsky, 2009; Long *et al.*, 2014). In plants, miRNAs are involved in developmental processes such as organ separation, leaf development, the establishment of polarity, lateral root formation, the development of floral organ identity and reproduction (Liu *et al.*, 2014, 2017; Zhang *et al.*, 2014; Wang *et al.*, 2015; Fal *et al.*, 2016; Merelo *et al.*, 2016). Additionally, miRNAs can respond to stresses (Sunkar & Zhu, 2004). Arabidopsis miR393 was the first miRNA discovered to be involved in plant immunity (Navarro *et al.*, 2006). Both miR160 and miR164 were induced when rice (*Oryza sativa*) was inoculated with *Magnaporthe oryzae* (Li *et al.*, 2014). In wheat (*Triticum aestivum* L.), miR393, miR444, miR827, miR2005, and miR2013 are up-regulated during interactions with the powdery mildew fungus *Blumeria graminis* (Xin *et al.*, 2010).

Although host endogenous sRNAs have been extensively studied in plant–pathogen interactions, pathogen-derived non-coding sRNAs have been recognized only recently. RNAi components (Dicer and Argonaute) have been identified in filamentous fungi (Fulci & Macino, 2007). Moreover, microRNA-like RNAs (milRNAs) have been reported in *Neurospora crassa* (Lee *et al.*, 2010), as well as in other filamentous fungi, including *Sclerotinia sclerotiorum* (Zhou *et al.*, 2012a), *Metarhizium anisopliae* (Zhou *et al.*, 2012b) and *Trichoderma reesei* (Kang *et al.*, 2013). Long terminal repeat (LTR) retro-transposon-siRNAs (LTR-siRNAs) and transfer RNA (tRNA) -derived RNA fragments (tRFs) from mycelial and appressorial tissue of *M. oryzae* were validated using 3′ rapid amplification of cDNA ends (RACE) PCR and northern blot analyses, respectively (Nunes *et al.*, 2011). Various physiological stressors and *in planta* conditions alter the sRNA profile of the rice blast fungus, and these sRNAs also play a role in transcriptional regulation of a subset of genes (Raman *et al.*, 2013). In addition, RNAi components and sRNAs have been identified in *Puccinia striiformis* f. sp. *tritici* (*Pst*; Mueth *et al.*, 2015).

Recently, attention has been focused on mobile sRNAs that mediate cross-kingdom RNAi in host–pathogen interactions (Weiberg & Jin, 2015). In plants, cotton increases production of miR166 and miR159 and export both to *Verticillium dahliae* fungal hyphae for specific silencing (Zhang *et al.*, 2016). Barley (*Hordeum vulgare*) C-14-α-demethylase (*CYP3*) dsRNA targets the three *Fusarium graminearum* cytochrome P450 lanosterol C-14α-demethylase genes to inhibit fungal growth (Koch *et al.*, 2016). In fungi, sRNAs can suppress plant immunity by hijacking host RNAi pathways (Weiberg *et al.*, 2013). In *Botrytis cinerea*, such sRNA effectors are mostly produced by Bc-Dicer-like protein 1 (DCL1) and Bc-DCL2 (Wang *et al.*, 2016). Fungal studies have uncovered surprisingly diverse sRNA biogenesis pathways, suggesting that fungi utilize RNAi-related pathways in various cellular processes to adapt to different environmental conditions (Weiberg & Jin, 2015).

Wheat stripe rust, which is caused by *Pst*, is among the most destructive wheat diseases in the world. Wheat yield can be greatly reduced or even completely destroyed at an epidemic level. Genetic control of wheat stripe rust is achieved by over 50 identified genes, formally named *Yellow rust* (*Yr*) *Resistance* (*R*) genes (Schwessinger, 2016). However, *Pst* can rapidly adapt and produce effectors that play important roles in pathogenicity, such as *Pst* effector candidate 6 (PEC6), which can suppress wheat defense reactions (Liu *et al.*, 2016). To expedite the study of the biology, epidemiology and virulence factors of this fungus, a *Pst* sRNA (germ tubes) library was constructed through the separation of small-sized RNA and high-throughput sequencing. Within this library, we found a novel milRNA, which was the most abundant sRNA in this library. In this study, we demonstrate that a novel milRNA in *Pst*, named *Pst*-milR1, regulates a target gene in wheat, and this target gene has been identified as a pathogenesis-related 2 (*PR2*) gene encoding a β-1,3-glucanase (EC3.2.1.39; Li *et al.*, 2001). We also suggest potential roles for *Pst* milRNAs in the pathogen–host interaction.

Materials and Methods

Plant material, inoculation, and treatments

Six Chinese *Puccinia striiformis* f. sp. *tritici* (wheat stripe rust) isolates (CYR23, CYR29, CYR31, CYR32, CYR33, and Su11-4), one US isolate (PST-78), one Pakistani isolate (PK-CDRD), two German isolates, two Australian isolates, one Kenyan isolate and one Ethiopian isolate were obtained from our laboratory (Cheng *et al.*, 2015; Luo *et al.*, 2015). Fresh *Pst* urediospores germinated to produce germ tubes in water (9°C for 12 h). Suwon 11 (Su11) is a Chinese wheat (*Triticum aestivum* L.) cultivar that is highly resistant to *Pst* CYR23 (incompatible interaction) and highly susceptible to CYR31 (compatible interaction). Wheat seedlings were grown, inoculated with *Pst*, and maintained following procedures and conditions previously described (Kang *et al.*, 2002). Inoculated and control wheat leaves were harvested at 0 (qRT-PCR for *Pst*-milR1 using urediospores as Mock) 24, 48, 72, and 120 h post inoculation (hpi) and immediately frozen in liquid nitrogen. Three independent biological replicates were performed for each treatment. Fresh *Pst* urediospores were collected for quantitative reverse transcriptase—polymerase chain reaction (qRT-PCR) and northern blot analyses. *Nicotiana benthamiana* (tobacco), which was used for co-transformation, was maintained at 25°C under a 16-h photoperiod.

For the chemical treatments, 4-wk-old Su11 seedlings were sprayed (0.1 ml per plant) with 2 mM salicylic acid (SA), 100 µM methyl jasmonate (MeJA), or 100 µM ethephon (ET) in 0.05% Tween 20. The control consisted of 0.05% Tween 20 (Liu *et al.*, 2010). Leaf samples (the second leaves) were harvested at 0, 0.5, 2, 6, 12, and 24 h post-treatment (hpt).

RNA extraction and sequencing data analysis

Total RNAs was extracted from germ tubes of the *Pst* isolate CYR32 using the mirVana miRNA isolation kit (Ambion, Austin, TX, USA) according to the manufacturer's instructions. sRNAs of *Pst* between 18 and 30 nucleotides were isolated using denatured polyacrylamide gel electrophoresis (PAGE); RNA oligonucleotides labeled at positions 18 and 30 were used as size standards. After ligation to the 5′ and 3′ adapters, the sRNAs were reverse transcribed to cDNA using RT-PCR. The PCR products were sequenced using an Illumina Genome Analyzer (BGI, Shenzhen, China). Final clean reads were obtained by deleting contaminant reads including 5′ primer contaminants, polyA, those without a 3′ primer, and insert tags. sRNA sequences were mapped to the *Pst* genome using the Short Oligo Alignment Program (SOAP; Li *et al.*, 2008). sRNAs with perfect genomic matches were used for further analysis. All trimmed sequences between 19 and 30 bp in length were used to search the Rfam database (10.1) using BLASTN to eliminate the sRNAs that originated from ribosomal RNA (rRNA), tRNA, small nuclear RNA (snRNA) and small nucleolar RNA (snoRNA) which were non-siRNA and non-miRNA sequences. We used the SHORTSTACK software package to identify miRNA loci (http://github.com/MikeAxtell/ShortStack). Then, we used the

pri-miRNA sequence to form hairpin structures using MFOLD (http://unafold.rna.albany.edu/?q=mfold).

RNA gel analysis of milRNA expression

Total RNA (100 μg) isolated from the CYR31 spores was run on a 15% denaturing urea-PAGE gel. RNA gel analysis was performed according to Wang *et al.* (2014). The RNA concentration was determined using a NanoDrop™ 1000 spectrophotometer (Thermo Fisher Scientific, Waltham, MA, USA).

Primer design, cDNA synthesis and DNA extraction

MicroRNA primers were designed and constructed using Feng's method (Feng *et al.*, 2012). To synthesize cDNA from RNA, a Revert Aid First-strand cDNA synthesis kit from Fermentas (Waltham, MA, USA) was used. Before reverse transcription (RT) of mature miRNAs, 3 μg of total RNA and 4.0 μl of primer mix (0.5 μl of each miRNA RT primer and 0.5 μl of the inner reference gene reverse transcription primer) were combined in a total volume of 10 μl with RNase-free water and incubated at 85°C for 5 min, followed by cooling on ice. Then, a 10-μl mix (6 μl of 5x RT-buffer (Invitrogen, Carlsbad, CA, USA), 2 μl of 2.5 mM dNTPs (Invitrogen), 1 μl of RNase inhibitor and 1 μl of Moloney Murine Leukemia Virus (M-MLV) RT enzyme 200 U (Invitrogen)) was added for a final volume of 30 μl.

The genomic DNA of 14 *Pst* isolates was extracted using the hexadecyl trimethyl ammonium bromide protocol (Murray & Thompson, 1980).

Polymorphism analysis

To identify intraspecific polymorphisms, precursors of *Pst*-milR1 were cloned from the genomic DNA of 14 *Pst* isolates. PCR amplification was performed with 50 ng of genomic DNA under the following conditions: 95°C for 4 min; 95°C for 30 s, 56°C for 30 s, and 72°C for 1 min (35 cycles), followed by 72°C for 10 min. The PCR product was ligated into the pGEM-T Easy vector for sequencing. *Puccinia graminis*, *Puccinia triticina*, *Melampsora larici-populina*, *Ustilago maydis*, *F. graminearum* and *Magnaporthe oryzae* gene sequences were downloaded from Ensembl Fungi (http://fungi.ensembl.org/index.html). *Uromyces fabae* gene sequences were obtained from the Voegele laboratory (Link *et al.*, 2014). Local blast searches using BIOEDIT software (http://www.mbio.ncsu.edu/BioEdit/bioedit.html) were carried out to identify the corresponding sequences using default settings (E-value $< e^{-5}$); the matrice was used PAM30. MEGA 5.0 software (http://www.megasoftware.net) was used to create multiple sequence alignments using default settings which were then manually adjusted.

Real-time quantitative PCR analysis

All quantitative PCRs were performed in a CFX96 Real-Time System (Bio-Rad, Munich, Germany) using SYBR Green I (Invitrogen). The total volume of PCR reactions was 25 μl. PCR conditions were as follows: 94°C for 1 min, 25 cycles of 94°C for 15 s, 55°C for 15 s, and 72°C for 1 min, followed by 72°C for 5 min. To standardize the data, translation elongation factor 1α of *Pst* (*PstEF-1a*) and wheat elongation factor *Ta*EF-1α were used as internal references for *Pst* and wheat qRT-PCR analysis, respectively. All primers used in the qRT-PCR are listed in Supporting Information Table S1. The qRT-PCR data were analyzed using the comparative $2^{-\Delta\Delta CT}$ method (Livak & Schmittgen, 2001).

Biomass analysis

To estimate changes in fungal biomass, the single-copy target genes rust transferred protein 1 (*PstRTP1*) and *TaEF1* were used to analyze the slopes of standard curves (Panwar *et al.*, 2013a). Total genomic DNA was used to prepare the standard curves. The correlation coefficients for the analysis of the serial dilutions were > 0.99. The relative quantities of the PCR products of *PstRTP1* and *TaEF1* in the infected samples were calculated using the gene-specific standard curves to quantify the respective *Pst* and wheat genomic DNA.

Prediction of miRNA targets

Pst gene sequences were downloaded from the National Center for Biotechnology Information (NCBI) (Zheng *et al.*, 2013). We used TARGETFINDER 1.6 software (https://github.com/carrington lab/TargetFinder) to search for targets in *Pst*. TARGETFINDER was run using the default settings and a score cut-off ≤ 4.0. Target gene prediction for *Pst*-milR1 was performed using the PSRNATARGET (http://plantgrn.noble.org/psRNATarget/) program. No gap or bulge within the alignment between sRNA and the target was allowed, and the 10th nucleotide of the sRNA was required to perfectly match its target. At most one mismatch or two wobbles were allowed from position 2 to 12. A maximum of two continuous mismatches was allowed, using a score cut-off 4.0.

Co-transformation of milRNAs and target genes in *N. benthamiana* leaves

Co-transformation of *N. benthamiana* leaves was used to validate the interaction between milRNAs and their respective target genes. Precursors of *Pst*-milR1 were cloned from CYR32 genomic DNA, and the target gene sequence, including the cleavage site, was cloned from the cDNA of wheat Su11. PCR amplification was performed with 50 ng of genomic DNA under the following conditions: 94°C for 5 min, 35 cycles of 94°C for 1 min, 58°C for 1 min, and 72°C for 2 min, followed by 72°C for 10 min. The PCR product was ligated into the pGEM-T Easy vector for sequencing. milRNA and the target gene were each integrated into the pBI121 vector, which contained the reporter gene β-glucuronidase (*GUS*). The precursor of *Pst*-milR1 was digested using the restriction endonucleases *Bam*HI and *Sac*I and cloned into the pBI121 vector. The region containing the cleavage site target sequences was digested using the restriction endonucleases *Xba*I and *Bam*HI and cloned into the pBI121 vector. If the

miRNA could cleave the target, the expression level of the *GUS* gene would be down-regulated. *Agrobacterium tumefaciens* strain GV3101 grown in Lysogeny broth medium at 28°C was used to introduce the recombinant vectors into *N. benthamiana* leaves. Strains carrying the different recombinant vectors (GV3101-pBI121, GV3101-pBI121-SM638, GV3101-pBI121-pre-Pst-milR1 and GV3101-pBI121-pre-Pst-milR1 + GV3101-pBI121-SM638) were cultured to an optical density of 0.8 at 600 nm (OD_{600}) before injection. The samples were diluted to $OD_{600} = 0.5$ using 10 mM $MgCl_2$ and 150 µM acetosyringone (Wang *et al.*, 2011). GV3101-pBI121 was selected as the control. The liquid (1 ml) from each treatment was infiltrated into the *N. benthamiana* leaves. Histochemical staining and GUS quantitative detection were conducted using three independent biological replicates as described by Jefferson *et al.* (1987).

The polyA region of the *SM638* gene was too short to design primers for RNA ligase-mediated 5′ RACE. We used the primers (Table S2) from the pBI121 vector to check the cleavage side in *N. benthamiana* leaves (GV3101-pBI121-pre-Pst-milR1 + GV3101-pBI121-SM638). Total RNA (10 µg) was used for RNA ligase-mediated (RLM) 5′ RACE (FirstChoice RLM-RACE Kit; Ambion), following the manufacturer's instructions. Degraded mRNAs with a 5′ RNA adaptor were used for reverse transcription. Subsequently, 1 µl of reverse transcription product was used to nest PCR, which was performed using a 5′ nested adaptor primer and a 3′ gene-specific nested primer (outer or inner primer). PCR amplification was performed based on the following conditions: 94°C for 3 min; 35 cycles of 94°C for 30 s, 60 °C for 30 s, and 72°C for 30 s, followed by 72°C for 10 min. The final PCR product was cloned into a pGEM-T Easy vector for sequencing.

BSMV-mediated *Pst*-milR1 gene silencing

Capped *in vitro* transcripts were prepared from linearized plasmids containing the tripartite barley stripe mosaic virus (BSMV) genome (Petty & Jackson, 1990) using the Message Machine T7 *in vitro* Transcription Kit (Ambion), following the manufacturer's instructions. RNA-derived clones (BSMV-*Pst*-milR1) were created using BSMV-TaPDS in which wheat phytoene desaturase (*TaPDS*) sequence fragments were replaced with specific *Pst*-milR1 sequences. BSMV-*Pst*-milR1 was prepared using a 197-bp specific fragment derived from the downstream precursor of *Pst*-milR1 without the mature sequences. In addition, a BLAST search of the fragments in GenBank showed no similarities with any other wheat gene. Following digestion with the restriction enzymes *Not*I and *Pac*I, the amplicon was directionally ligated into the *Not*I/*Pac*I sites of the BSMV:γ vector. At the two-leaf stage, wheat seedlings were infected with BSMV using the method described by Hein *et al.* (2005). The wheat seedlings were inoculated with each of the three viruses (BSMV:γ, BSMV:*TaPDS*as and BSMV:*Pst*-milR1as). BSMV:*TaPDS*as was used as a positive control. The second leaf of a two-leaf wheat seedling was inoculated with BSMV transcripts by gently rubbing the surface with gloved fingers, followed by incubation at 25°C and subsequent examination for symptoms at regular intervals. Ten days after

virus inoculation, the fourth leaf was infected with urediospores of CYR23 (avirulent) or CYR31 (virulent). The fourth leaves were sampled at 0, 24, 48, and 120 hpi for RNA isolation and cytological observation. Analysis by qRT-PCR was used to calculate the silencing efficiency of *Pst*-milR1 (Yin *et al.*, 2015). *Pst* infection phenotypes were recorded and photographed at 14 d post inoculation (dpi). The method of silencing *SM638* and *Pst* Dicer-like protein (*PsDCL*) was the same as for *Pst*-milR1. The primers used for all plasmid constructions are presented in Table S2.

Histological observation of fungal growth

Harvested samples were decolorized as described previously (Wang *et al.*, 2007). For better visualization of internal infection structures, the staining procedure for wheat germ agglutinin (WGA) conjugated to the fluorophore alexa 488 was also used (Invitrogen). Leaf segments cut from the transparent wheat leaves were examined using an Olympus BX-51 microscope (Olympus Corp., Tokyo, Japan). For each treatment, at least 50 different infection sites were examined on each of five randomly selected leaf segments. Hyphal length and infection area were calculated using DP-BSW software (Olympus Corp., Tokyo, Japan). SPSS software (SPSS Inc., Chicago, IL, USA) was used to calculate the standard deviations and to perform Tukey tests for the statistical analyses.

Data availability

The data are in the NCBI Sequence Read Archive, accession SRR5078242.

Results

Identification of milRNA1 in *Pst*

To comprehensively examine sRNAs in *Pst*, an sRNA library of *Pst* CYR32 germ tubes was prepared using a high-throughput sequencing technology. Three biological replicates were carried out. A total of 18.3 million raw reads ranging in size from 17 to 30 nt were generated. After removing low-quality and adaptor sequences, 14.9 million clean reads were generated (Table S3). We used BLAST of sRNAs against the Rfam database to remove noncoding RNAs such as rRNA, tRNA, snRNA and snoRNA. A total of 608 potential sRNAs were obtained by bioinformatic analysis, with sequences exactly matching the *Pst* genome. To identify potential milRNA in *Pst*, we applied the SHORTSTACK software package to identify miRNA loci. Then, we formed hairpin structures with the pri-miRNA sequences using MFOLD to identify potential milRNAs. Within the sRNA library, we found a novel milRNA with 10 534 reads that was highly expressed, which we named *Pst*-milR1 (KY275365). *Pst*-milR1 encodes a mature sequence of 20 bp, which starts with a U. The 231-bp precursor of *Pst*-milR1 is novel, with sequences exactly matching the *Pst* genome but not the wheat genome or wheat cDNA. We predicted that the precursor of *Pst*-milR1 could form a hairpin structure, which meets most but not all miRNA criteria for

animals and plants (Meyers *et al.*, 2008). The mature sequence of *Pst*-milR1 was generated from the 5′ end of the precursor (Fig. S1).

To identify *Pst*-milR1 in *Pst*, we analyzed the accumulation of *Pst*-milR1 from urediospores and germ tubes using northern blotting. The results showed that *Pst*-milR1 was present in both cell structures (Fig. 1a). However, we did not find *Pst*-milR1 in wheat or Arabidopsis (Fig. 1b).

To determine whether there is an intraspecific polymorphism in *Pst*-milR1, we cloned its precursor sequence from 14 different *Pst* isolates, including six Chinese isolates, one US isolate, two German isolates, two Australian isolates, one Kenyan isolate, one Ethiopian isolate and one Pakistani isolate, using PCR. We found that *Pst*-milR1 was highly conserved, as there were no nucleotide substitutions in its precursor in all 14 isolates. Moreover, we also checked for the presence of this precursor sequence in other plant pathogenic fungi, including *P. graminis*, *P. triticina*, *U. fabae*, *M. larici-populina*, *U. maydis*, *F. graminearum* and *M. oryzae*. No such sequence could be identified in any of the plant pathogenic fungi analyzed. Thus, our results suggest that *Pst*-milR1 may be a unique *Pst* milRNA.

Pst-milR1 regulates the target gene *PR2* in *N. benthamiana* leaves

miRNAs are reported to play essential roles in regulating corresponding target genes (Lau *et al.*, 2013). We predicted the candidate targets in the *Pst* genome using bioinformatics analysis. However, we were not able to identify a suitable target of *Pst*-milR1 in *Pst*. Fungal sRNAs could also trigger silencing of host genes that are likely to function in plant immunity (Weiberg *et al.*, 2013). Therefore, we predicted target genes in wheat to test whether *Pst*-milR1 could suppress host genes during infection. The polyA region of a beta-1,3-glucanase (*SM638*) was identified as a potential target of *Pst*-milR1 (Table S4). SM638 has been reported to be a new type of β-1,3-glucanase, which belongs to the *PR2* gene class in wheat (Li *et al.*, 2001). From the NCBI, we
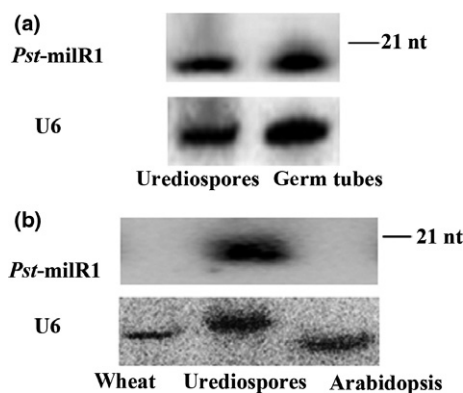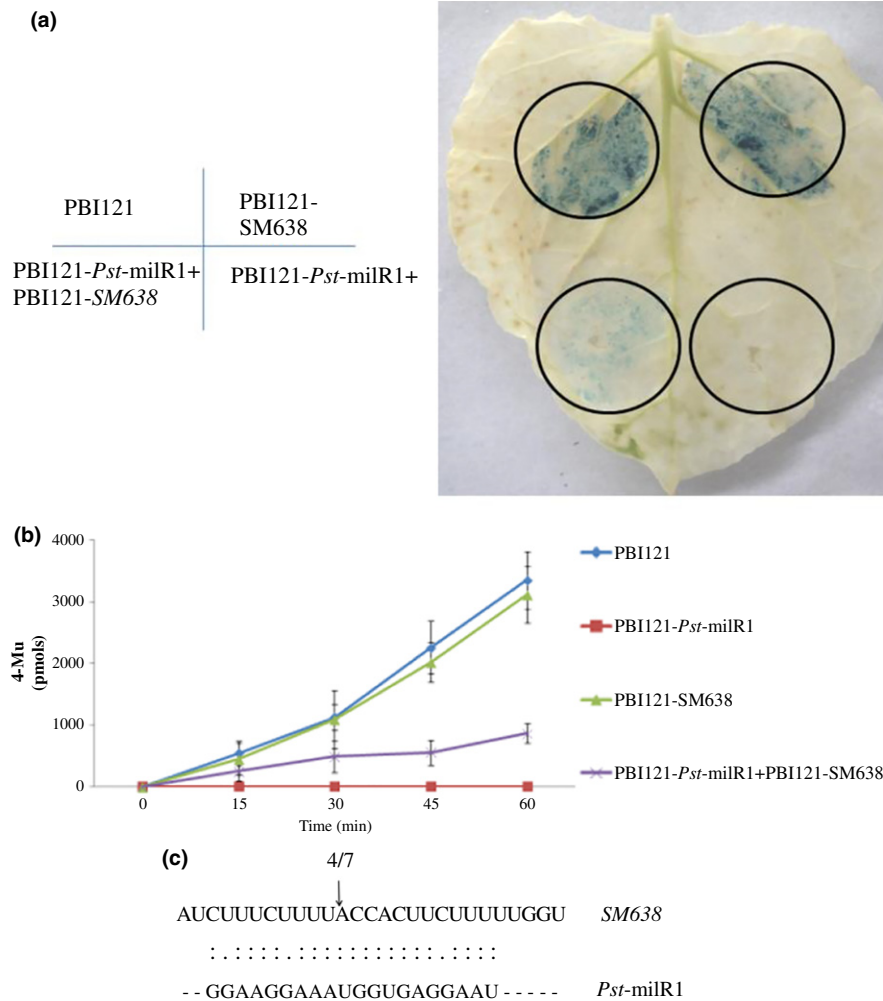
selected nine wheat homologous *PR2* genes. Using sequence alignments, we predicted that *Pst*-milR1 could bind *SM638* but not any other wheat *PR2* genes (Fig. S2). To verify the suppression of the target by *Pst*-milR1, we applied co-transformation technology to *N. benthamiana* (Fig. 2a). The recombinant vector pBI121 containing *GUS* as a reporter gene was introduced into cells of *N. benthamiana* leaves using the *A. tumefaciens*-mediated transformation system. Control leaves infiltrated with GV3101-pBI121 were observed for the GUS phenotype by histochemical staining. Leaves infiltrated with GV3101-pBI121-SM638, in which the target sequence was fused upstream of the *GUS* gene, showed a similar phenotype. In leaves infiltrated with GV3101-pBI121-pre-*Pst*-milR1, in which the *GUS* gene was replaced by the precursor of *Pst*-milR1, the GUS phenotype was not observed. GUS staining was markedly reduced in leaves co-transformed with the strain mixture GV3101-pBI121-SM638 and GV3101-pBI121-pre-*Pst*-milR1. This was considered as additional evidence that *Pst*-milR1 could target *SM638*.

To confirm the results of these histochemical observations, the amount of GUS in each leaf was assessed using a fluorospectrophotometer (Fig. 2b). Fluorescence was determined in all four samples at different time-points. We found that the fluorescence of GV3101-pBI121 (control) and GV3101-pBI121-SM638 was enhanced by extending the reaction time in the inoculated leaf samples, which indicates that GUS was still present and functional. Almost no fluorescence was detected in leaves injected with GV3101-pBI121-*Pst*-milR1. Compared with the control, fluorescence of the strain mixture (GV3101-pBI121-SM638 and GV3101-pBI121-pre-*Pst*-milR1) exhibited a slower increase. These results demonstrate that *Pst*-milR1 effectively regulated the target gene.

To further confirm the co-transformation results, we carried out 5′ RACE PCR in *N. benthamiana* leaves injected with the strain mixture (GV3101-pBI121-SM638 and GV3101-pBI121-pre-*Pst*-milR1). The 5′-RACE PCR product, which was detected using gel electrophoresis, was sequenced. From seven cloned RACE products, four sequencing results showed that the validated cleavage site was lagging between the 11th and 12th nucleotides. We found that *SM638* could be cleaved by *Pst*-milR1 (Fig. 2c).

SM638 is regulated by *Pst*-milR1 in a wheat–*Pst* compatible interaction

To explore the role of *Pst*-milR1 in pathogenicity, we examined the transcript levels of the predicted target gene and *Pst*-milR1 in *Pst*-infected wheat leaves at 0 (*Pst* urediospores, germ tubes) were used for qRT-PCR of miR1, not for target gene, 24, 48, 72 and 120 h. The results from our qRT-PCR experiments showed that the *Pst*-milR1 transcript levels increased slightly when wheat (Su11) was challenged with either *Pst* race (CYR31 (virulent) or CYR23 (avirulent)). In particular, *Pst*-milR1 accumulation increased at 24 and 48 hpi in the compatible interaction (Fig. 3a). In the incompatible interaction, the *SM638* transcript levels increased at 24 hpi and exhibited a *c.* 4.7-fold peak response at 120 hpi. The accumulation of *Pst*-milR1 increased slightly in the

Fig. 1 Identification of *Puccinia striiformis* f. sp. *tritici* microRNA-like RNA 1 (*Pst*-milR1) in different plant tissue and fungal cell types. (a) *Pst*-milR1 is expressed in urediospores and germ tubes of CYR31. (b) Detection of *Pst*-milR1 in *Pst*, but not wheat or Arabidopsis. Total RNA (100 μg) was used for northern blot analysis. The small nuclear RNA U6 was used as a loading control.

Fig. 2 Co-transformation of *Puccinia striiformis* f. sp. *tritici* microRNA-like RNA 1 (*Pst*-milR1) and *SM638* into *Nicotiana benthamiana* leaves. (a) β-Glucuronidase (GUS) phenotype observed by histochemical staining. (b) Quantitative detection of GUS activity in leaves inoculated with different recombinant vectors at different time-points using a fluoro-spectrophotometer. 4-MU, 4-methyl-umbelliferyl-β-D-glucuronide. (c) Validation of the *Pst*-milR1 target gene by RNA ligase-mediated (RLM) 5′ rapid amplification of cDNA ends (RACE). The black arrow indicates a cleavage site verified by RLM 5′-RACE, with the frequency of cloned RACE products shown above the alignment. All treatments were performed in duplicate. Results are composed of the mean ± SE of three biological replications.

germ tubes of the CYR31 isolate. By contrast, the transcript levels of *SM638* decreased slightly in the compatible interaction (Fig. 3b). These data suggest that *Pst*-milR1 is negatively correlated with *SM638* in a compatible interaction, which is consistent with its function in binding the target *in planta*.

We also tested the expression of *SM638* under JA, SA, and ET stress. The *SM638* transcript levels were strongly elevated, reaching *c.* 4.3- and 3.1-fold peaks at 0.5 hpt in response to SA and JA, respectively. By contrast, the transcript levels of *SM638* were not affected by the ET treatment (Fig. 3c). These results suggest that SA/JA signaling may be involved in *SM638* regulation.

Knocking down *Pst*-milR1 reduces the virulence of *Pst*

To test the role of *Pst*-milR1 during wheat–*Pst* interactions, we silenced *Pst*-milR1 using the host-induced gene silencing

(HIGS) system (Nowara *et al.*, 2010; Panwar *et al.*, 2013a,b). We silenced *Pst*-milR1 in the wheat cultivar Su11, which is susceptible to *Pst* isolate CYR31, using BSMV-mediated HIGS (Fig. 4a). As a control to confirm that the RNAi system was functional, we silenced the wheat phytoene desaturase (*PDS*) gene through inoculation with the recombinant virus BSMV:*TaPDS*as, which showed a photobleaching phenotype at 15 dpi. None of the BSMV-inoculated plants showed any obvious defects in further leaf growth. BSMV:γ leaves inoculated with CYR31 produced numerous urediospores at 15 dpi. Compared with BSMV:γ leaves, limited urediospore production was observed on leaves infected with BSMV:*Pst*-milR1. qRT-PCR was used to calculate the silencing efficiency of *Pst*-milR1. As a control to confirm that the RNAi system was functional, qRT-PCR showed that the expression of *PDS* was suppressed (Fig. S3). Compared with leaves inoculated with
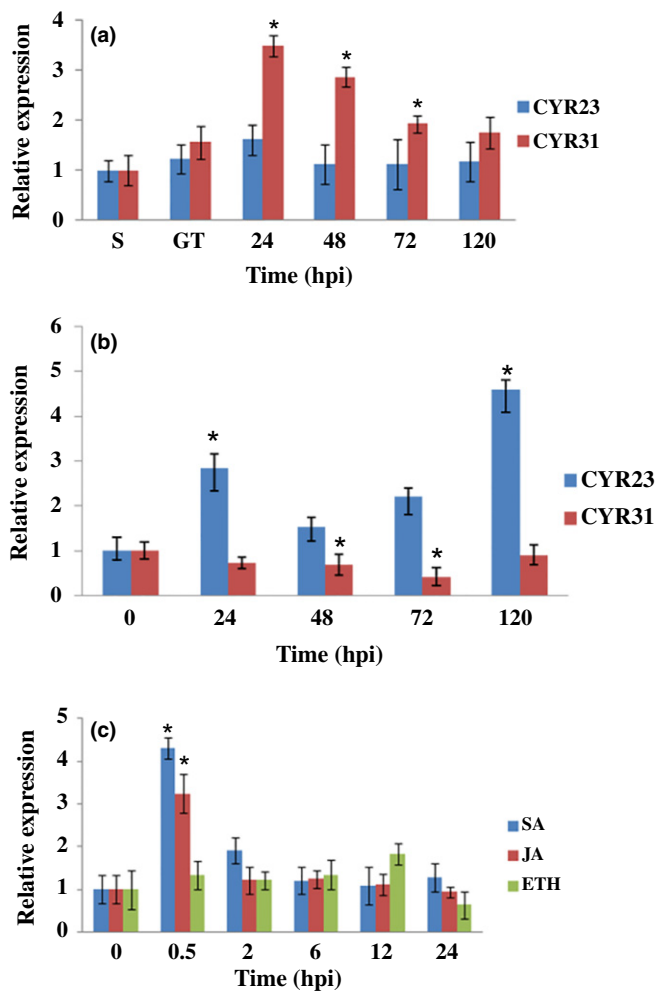
Fig. 3 Transcript levels of *Puccinia striiformis* f. sp. *tritici* microRNA-like small RNA 1 (*Pst*-milR1) and *SM638*. (a) Transcript profiles of *Pst*-milR1 in wheat leaves (Su11) inoculated with *Pst* race CYR31 (virulent). (b) The relative the transcript levels of *SM638* in wheat leaves (Su11) inoculated with *Pst* races CYR31 (virulent) and CYR23 (avirulent), respectively. (c) *SM638* transcript profiles in wheat leaves treated with abiotic stress. Mean expression values were calculated from three independent replicates. Bars represent ± SD. Significant differences were determined using Student's *t*-test: *, $P < 0.05$. S, urediospores; GT, germ tubes; hpi, h post inoculation; hpt, h post treatment; SA, salicylic acid; JA, methyl jasmonate; ETH, ethylene.

BSMV:γ, the average transcript level of *Pst*-milR1 was knocked down in the leaves inoculated with BSMV:*Pst*-milR1 by 73, 67 and 57% at 24, 48 and 120 hpi, respectively (Fig. 4b; Table S5). The relative transcript levels of *SM638* were also analyzed in *Pst*-milR1 knocked-down leaves. The transcript levels of *SM638* were significantly up-regulated in *Pst*-milR1 knocked down leaves challenged with CYR31 (Fig. 4c), but the transcript levels of the other *PR2* did not show obvious changes (Fig. S4). The *Pst* biomass was also reduced in the *Pst*-milR1 knocked-down leaves (Fig. 4d). These results indicate that silencing of *Pst*-milR1 may affect *SM638* expression.

Compared with the control, wheat leaves inoculated with BSMV:*Pst*-milR1 limited urediospore production of CYR31. To

further verify this phenotype, detailed histological changes in *Pst*-milR1 knocked-down and control plants were measured (Table 1). At 24 and 48 hpi, significant differences in the number of hyphal branches and haustorial mother cells were observed. Moreover, the infection area in wheat leaves pre-inoculated with BSMV:*Pst*-milR1 was significantly ($P < 0.05$) reduced at 24 hpi. *Pst* hyphal length in wheat leaves pre-inoculated with BSMV:*Pst*-milR1 was also significantly ($P < 0.05$) shorter at 24 and 48 hpi.

SM638 improves wheat resistance to *Pst* in an incompatible interaction

To determine whether *SM638* is involved in host immunity, we applied the virus-induced gene silencing (VIGS) approach to knock down *SM638* in wheat Su11 challenged with *Pst* CYR23 (incompatible interaction) and CYR31 (compatible interaction) (Fig. 5a). Fresh urediospores of CYR23 and CYR31 were inoculated onto the surface of fourth leaves at 12 d post-virus inoculation. At 14 dpi with *Pst*, obvious hypersensitive response (HR) was elicited on the leaves of both the control check (CK) and BSMV-γ seedlings inoculated with CYR23, whereas seedlings with *SM638* knocked down (BMSV-SM638) displayed some sporulation (Fig. 5a). *SM638*-silenced wheat leaves challenged with CYR31 were not significantly affected. In the incompatible interaction, transcript levels of *SM638* were decreased by 59–68% (Fig. 5b). In the compatible interaction, expression of *SM638* was reduced by 66–77% (Fig. 5c). However, transcript levels of the other seven *PR2* genes tested were not affected (Fig. S5). The number of hyphal branches, the number of haustorial mother cells, the infection area size, and *Pst* hyphal length also increased in the incompatible interaction (Table S6).

Dicer-dependent biogenesis of milRNA in *Pst*

Most sRNAs are generated from dsRNA by the ribonuclease III enzyme Dicer (Navarro *et al.*, 2006). In the NCBI database, we found only one RNase III Dicer-like protein in *Pst*, named *PsDCL* (JN033211.1). To investigate the biological relevance of *Pst*-milR1 and *PsDCL*, transcript accumulation of *PsDCL* in wheat challenged with *Pst* was analyzed. The transcripts of *PsDCL* increased at 24 hpi and exhibited an approximate 10.6-fold peak at 72 hpi, before declining to a two-fold level at 120 hpi (Fig. 6a). To identify the function of *PsDCL* in wheat during *Pst* infection, we also constructed HIGS vectors to silence *PsDCL*. Compared with the BSMV-γ inoculated leaves, the transcript levels of *PsDCL* decreased by 42–78% (Fig. 6b). The *Pst*-milR1 transcript levels were also reduced at 24, 48, and 120 hpi (Fig. 6c). There was no obvious infection phenotypic change in the *PsDCL* knocked-down leaves during *Pst* infection (Fig. S6). However, the number of hyphal branches, number of haustorial mother cells and *Pst* hyphal length in wheat leaves pre-inoculated with BSMV-*PsDCL* were significantly ($P < 0.05$) reduced compared with wheat leaves pre-inoculated with BSMV-γ at 24 hpi (Table 2). This suggests that *PsDCL* might contribute to *Pst* virulence, as well as regulate accumulation of *Pst*-milR1.
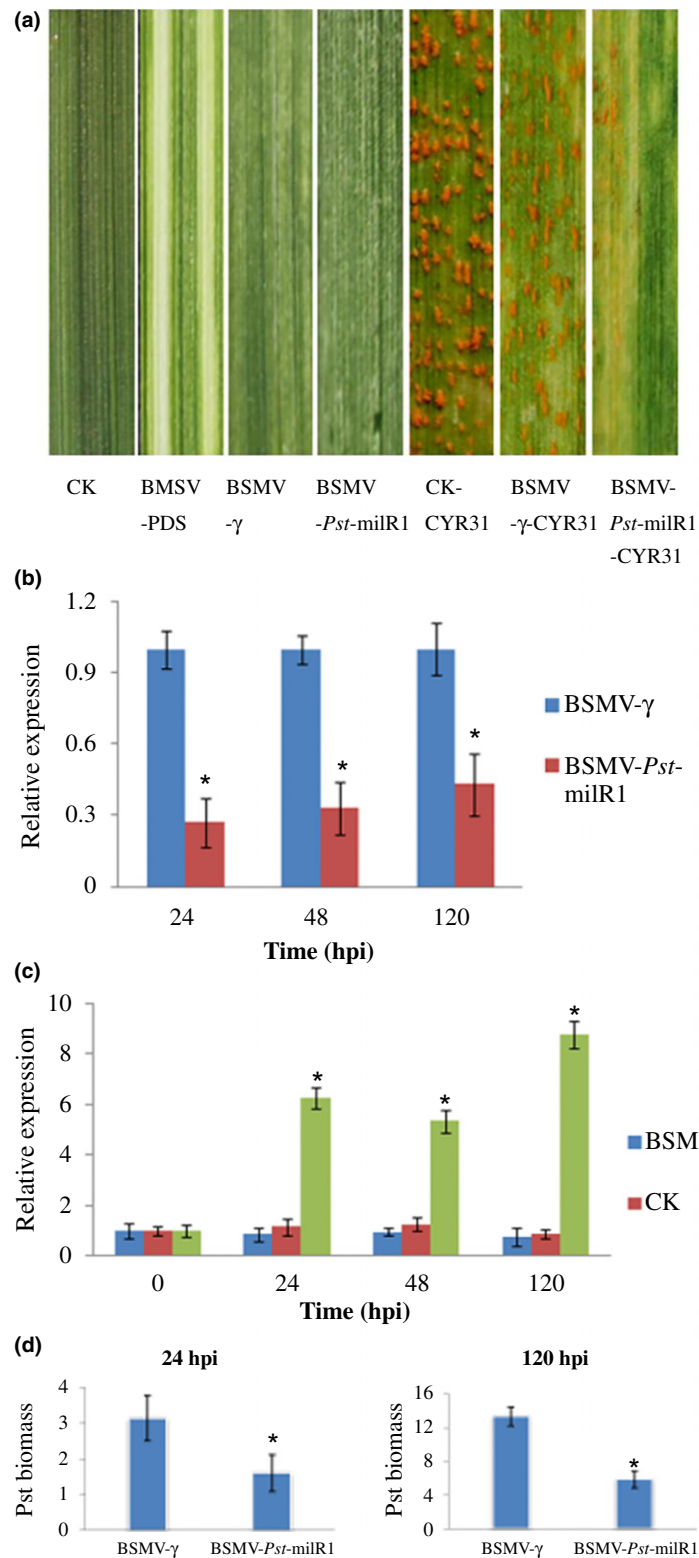
Fig. 4 Functional assessment of *Puccinia striiformis* f. sp. *tritici* microRNA-like RNA 1 (*Pst*-milR1) in the wheat–*Pst* interaction by host-induced gene silencing (HIGS). (a) Phenotypic differences among fourth leaves in plants pre-inoculated with control check (CK), FES buffer (sodium-pyrophosphate 1% (w/v), malacoid 1% (w/v), celite 1% (w/v), glycine 0.5 M, K 2 HPO 4 0.3 M, pH 8.5, with phosphoric acid), positive control vector (barley stripe mosaic virus−phytoene desaturase (BSMV-PDS)), empty BSMV vector (BSMV-γ), and BSMV-*Pst*-milR1 at 14 d post-virus treatment. Phenotypes of fourth leaves inoculated with CYR31 on plants whose second leaves were pre-injected with empty vector or BSMV-*Pst*-milR1 were observed at 14 d post inoculation (dpi). (b, c) Transcript levels of *Pst*-milR1 (b) and the target gene (c) in *Pst*-milR1 knocked-down leaves challenged with CYR31. (d) Biomass of *Pst* measured at 24 and 120 hpi. Means ± SD were calculated from three independent replicates. Significant differences were determined using Student's *t*-test: *, $P < 0.05$. hpi, h post inoculation.

Table 1 Histological analysis of *Puccinia striiformis* f. sp. *tritici* microRNA-like RNA 1 (*Pst*-milR1) knocked-down leaves of Su11 challenged with *Pst* CYR31

Treatment*	*Pst* hyphal length[†]		*Pst* hyphal branches[‡]		*Pst* infection area[‡]		Number of *Pst* HMCs[‡]
	24 hpi	48 hpi	24 hpi	48 hpi	24 hpi	48 hpi	24 hpi
BSMV-γ	0.27a ± 0.11	0.36a ± 0.05	2.36a ± 0.15	3.12a ± 0.13	0.31a ± 0.11	0.52a ± 0.09	2.09a ± 0.23
BSMV-*Pst*-milR1	0.19b ± 0.09	0.26b ± 0.07	1.83b ± 0.21	2.67b ± 0.32	0.24b ± 0.06	0.48a ± 0.04	1.67b ± 0.27

BSMV, barley stripe mosaic virus; hpi, hours post-inoculation; HMC, haustorial mother cell. Values within the same column marked with different superscript letters were significantly different ($P < 0.05$).
*Leaves were inoculated with BSMV:γ and BSMV:*Pst*-milR1, followed by inoculation with *Pst* CYR31.
[†]Average distance from the base of the substomatal vesicle to the hyphal tip calculated from at least 50 infection sites (measured in 10-mm units using Dp-bsw software).
[‡]All data are the average calculated from at least 50 infection sites. Tests of significance were based on paired sample *t*-tests using Spss software ($P < 0.05$).
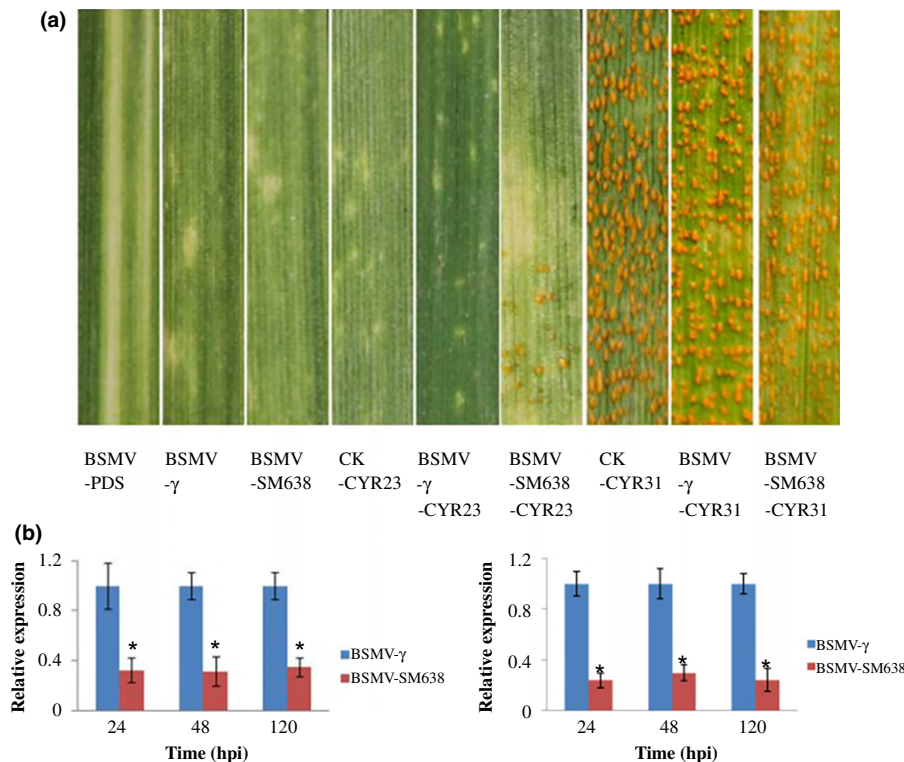

Fig. 5 Phenotypic changes on wheat leaves of *SM638* knocked-down plants and analysis of the silencing efficiency of *SM638*. (a) Phenotypic changes of fourth leaves in plants pre-inoculated with control check (CK), FES buffer (sodium-pyrophosphate 1% (w/v), malacoid 1% (w/v), celite 1% (w/v), glycine 0.5 M, K₂HPO₄ 0.3 M, pH 8.5, with phosphoric acid), empty barley stripe mosaic virus (BSMV) vector (BSMV-γ), or positive control vector (BSMV−phytoene desaturase (PDS)) at 14 d post-virus treatment. Phenotypes of the fourth leaves inoculated with *Pst* race CYR23 or CYR31 on plants whose second leaves were pre-injected with FES buffer, empty BSMV vector and BSMV-SM638 were observed at 14 d post inoculation. (b, c) Relative transcript levels of *SM638* in *SM638* knocked-down leaves challenged with race CYR23 (b) or CYR31 (c). Means ± SD were calculated from three independent replicates. Significant differences were determined using Student's *t*-test: *, $P < 0.05$. hpi, h post inoculation.

Discussion

Since the discovery of the first miRNA in *Caenorhabditis elegans* (Lee *et al.*, 1993), miRNAs have been found in diverse organisms, including animals, plants, and algae. However, only a few sRNAs have been identified in fungal pathogens. In this study, we identified a *Pst* miRNA-like RNA named *Pst*-milR1, which was highly up-regulated during wheat–*Pst* interactions. milRNA is a class of sRNAs in fungi that lack a common ancestor or functional conservation among different species (Weiberg *et al.*, 2014). *Pst*-milR1 is only found in *Pst*; it is not even found in other rust fungi such as *P. graminis* and *P. triticina*. Moreover, *Pst*-milR1 is conserved in different isolates of *Pst*. We infer that the formation of *Pst*-milR1 may be a result of *Pst* evolution and adaptation to the host plant.

miRNAs are important mRNA degradation regulators of target genes at the post-transcriptional level (Jones-Rhoades *et al.*, 2006). Research on the function of targets is very important to resolve miRNA regulation networks. Using Solexa sequencing and northern blot analysis, we found that *Pst*-milR1 was expressed at high levels in urediospores and germ tubes. However, we were not able to predict a suitable target of *Pst*-milR1 in
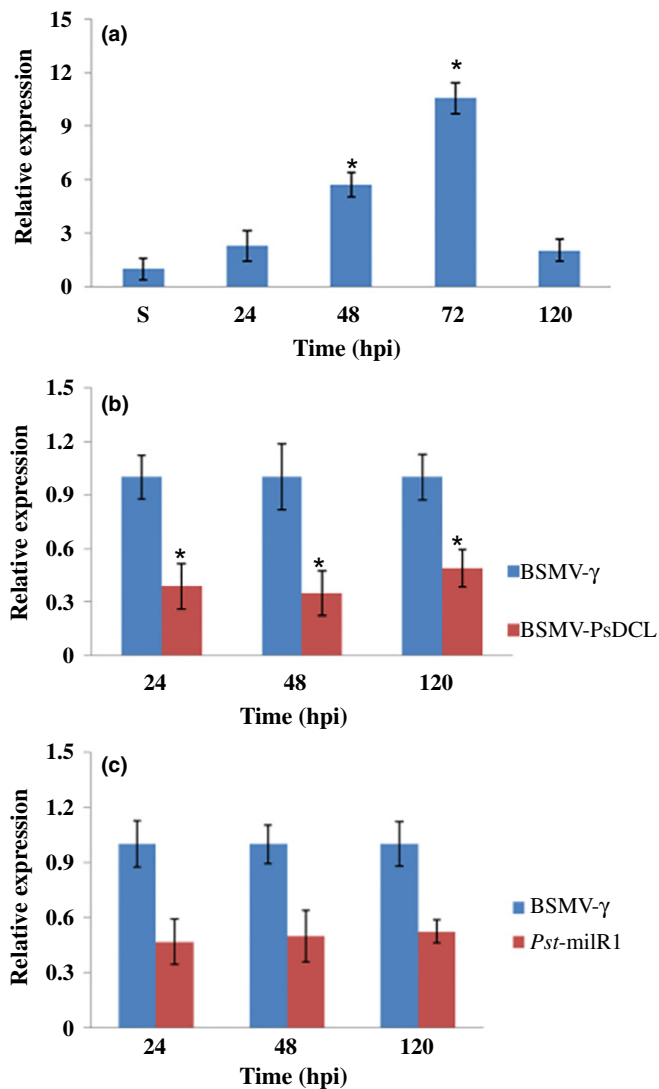
Fig. 6 Analysis of the silencing efficiency of *Pst* Dicer-like protein (*PsDCL*). (a) Transcript profiles of *PsDCL* in wheat leaves inoculated with *Pst* race CYR31. S, urediospores. (b, c) Transcript levels of (b) *PsDCL* and (c) *Puccinia striiformis* f. sp. *tritici* microRNA-like RNA 1 (*Pst*-milR1) in *PsDCL* knocked-down leaves challenged with race CYR31. Means ± SD were calculated from three independent replicates. Significant differences were determined using Student's *t*-test: *, $P < 0.05$.

Pst. Of course, we cannot rule out the possibility that we did not identify the target of *Pst*-milR1 in *Pst* because of the limitation of the current information and prediction technology. Nevertheless, the most interesting finding is that we have identified a target of *Pst*-milR1 from wheat, the host of *Pst*. Currently, accumulating evidence supports the notion that sRNAs can translocate between pathogens and host cells and can induce cross-kingdom RNAi: *Botrytis cinerea* sRNAs provide an excellent example of cross-kingdom RNAi by hijacking host Argonaute 1 (AGO1) and selectively silencing host immunity genes (Weiberg *et al.*, 2013). In this study, we found that *Pst*-milR1 could bind to a *PR2* transcript (β-1,3-glucanase) in wheat. The target sites of *Pst*-milR1 were similar to wheat miRNAs, which are in 3′ UTRs (Yao *et al.*, 2007). Co-transformation and 5′ RACE PCR results demonstrated that *Pst*-milR1 can regulate the expression of β-1,3-glucanase (*SM638*). Thus, these data suggest that *Pst*-milR1 may take part in cross-kingdom RNAi.

Fungi that colonize plants are recognized by the plant immune system and elicit host defenses. These defense responses are triggered by pathogen-associated molecular patterns (PAMPs), including the accumulation of antimicrobial compounds (Lo Presti *et al.*, 2015). These compounds include pathogenesis-related (PR) proteins, such as proteinases, chitinases, and glucanases, which damage pathogen structures (Muthukrishnan *et al.*, 2001). They have been classified into several groups based on their amino acid sequences and biochemical functions (Bowles, 1990). For example, beta-1,3-glucanases have been categorized as *PR2* genes. They are well known as hydrolytic enzymes that inhibit the growth of many fungi by hydrolyzing β-glucan in the fungal cell wall, followed by the release of elicitors from the decaying fungal cell wall that stimulate systemic acquired resistance (SAR) in the host plant (Bartnicki-Garcia, 1968; Mauch & Staehelin, 1989; Sela-Buurlage *et al.*, 1993). *PR2* genes are associated with SA-regulated defense responses. In the present study, the *PR2* gene *SM638* was over-expressed in wheat leaves upon treatment with SA. *PR2* genes have been identified as important defense-regulated genes. Pathogen-induced accumulation of β-1,3-glucanase has been reported in cereals. For example, Li *et al.* (2001) identified SM638 as a PR2 protein, for which the mRNA levels were much higher in spikes inoculated with a conidial

Table 2 Histological analysis of *Pst* Dicer-like protein (*PsDCL*) knocked-down leaves of Su11 responding to CYR31

| Treatment* | *Pst* hyphal length[†] | | *Pst* hyphal branches[‡] | | *Pst* infection area[‡] | | Number of *Pst* HMCs[‡] |
	24 hpi	48 hpi	24 hpi	48 hpi	24 hpi	48 hpi	24 hpi
BSMV-γ	0.24a ± 0.13	0.41a ± 0.07	2.23a ± 0.13	3.03a ± 0.21	0.35a ± 0.09	0.57a ± 0.11	2.32a ± 0.17
BSMV-*PsDCL*	0.17b ± 0.09	0.39a ± 0.05	1.63b ± 0.24	2.56a ± 0.27	0.32a ± 0.06	0.53a ± 0.07	1.53b ± 0.12

BSMV, barley stripe mosaic virus; hpi, hours post-inoculation; HMC, haustorial mother cell; *Pst*, *Puccinia striiformis* f. sp. *tritici*. Values within the same column marked with different superscript letters were significantly different ($P < 0.05$).
*Leaves were inoculated with BSMV:γ, or BSMV:*PsDCL*, followed by inoculation with *Pst* CYR31.
[†]Average distance from the base of substomatal vesicles to hyphal tips calculated from at least 50 infection sites (measured in 10-mm units using Dᴘ-ʙsᴡ software).
[‡]All data are the average number calculated from at least 50 infection sites. Tests of significance are based on paired sample *t*-tests using Sᴘss software ($P < 0.05$).

suspension of *F. graminearum* than in mock-inoculated controls. Liu *et al.* (2010) demonstrated that transcription of β-1,3-glucanase (*TaGlu*) was induced during both compatible and incompatible interactions with *Pst*. To further validate the function of β-1,3-glucanase, we repressed the expression of *SM638* in wheat by VIGS technology. When *SM638* was silenced in the incompatible interaction, wheat exhibited enhanced susceptibility to CYR23 and displayed some sporulation. Accordingly, we found that, while the expression of *SM638* was inhibited, *Pst*-milR1 was highly induced in the compatible interaction. Knockdown of *Pst*-milR1 increased the resistance of wheat to *Pst*. The infection area and hyphal length of *Pst* in wheat were significantly limited in the early stage of infection. However, the expression of the *SM638* gene was obviously up-regulated. These data suggest that *SM638*, as a *PR2* gene, might contribute to the wheat response to *Pst* but is regulated by *Pst*-milR1 in the process of *Pst* infection.

In general, pathogens deliver effector proteins into plant cells to suppress host PAMP-triggered immunity (PTI). In response, plant resistance proteins sense effectors to activate effector-triggered immunity (ETI), which is a second inducible defense layer. sRNAs of pathogens play important roles in challenging the ETI of plants. On the one hand, pathogen sRNAs can indirectly contribute to virulence by regulating the expression levels of effectors. For example, sRNAs regulate the effector gene Avirulence Conferring Enzyme1 (*ACE1*) in *M. oryzae*, which controls the initiation of appressorial penetration (Fudal *et al.*, 2007; Raman *et al.*, 2013). In addition, Qutob *et al.* (2013) reported that gene-silenced avirulence gene (Avr) strains could produce sRNAs to escape detection by host immune systems, but strains with Avr3a mRNA could not. On the other hand, pathogen sRNAs can function directly as effectors. Recently, it was reported that some Arabidopsis resistance genes were targeted in the coding regions and were suppressed after *B. cinerea* infection. For example, mitogen-activated protein kinase 2 (MPK2) and MPK1 are targeted by Bc-siR3.2. The *mpk1 mpk2* double mutant exhibited enhanced susceptibility to *B. cinerea* (Weiberg *et al.*, 2013). In this study, the results also show that *Pst*-milR1 may function as an effector, contributing directly to virulence by overcoming plant defense responses.

Cross-kingdom RNAi is a form of communication between unrelated species from different kingdoms, such as a host and its pathogen, pest, parasite, or symbiont (Weiberg & Jin, 2015). Cross-kingdom RNAi has been observed in plant systems that transfer RNAi signals into interacting organisms. For example, cotton plants export miR166 and miR159 to *V. dahliae* fungal hyphae for specific silencing (Zhang *et al.*, 2016). How does cross-kingdom RNAi occur? Recently, it was reported that *Heligmosomoides polygyrus* sRNAs were selectively sorted into exosomal vesicles for secretion via exocytosis (exosomes) (Buck *et al.*, 2014). *Heligmosomoides polygyrus* vesicles can be internalized by mice cells. One hypothesis regarding RNA signals in extracellular vesicles is that the intact vesicle can be endocytosed at the plasma membrane, after which the RNA will end up behind two membranes in an endosome (Knip *et al.*, 2014). However, there are also many mysteries

concerning sRNA transport in cross-kingdom RNAi. Thus, the exact mechanism of sRNA transport in cross-kingdom RNAi is an important area for future research.

The biogenesis of most miRNAs requires the participation of Dicer proteins (Lee *et al.*, 2010). A recent study reported that there are diverse pathways in the generation of milRNAs and Dicer-independent small interfering RNAs (disiRNAs) in *N. crassa* (Lee *et al.*, 2010). Most of the disiRNA-producing loci yield overlapping sense and antisense transcripts. In this respect, *Pst*-milR1 shares similar characteristics to miRNAs in animals and plants, with highly specific stem-loop RNA precursors. DCL is involved in pathogenesis in some plant pathosystems. For example, *PiDCL1* in *P. infestans* was highly induced at 24 hpi (Weiberg *et al.*, 2014). *Botrytis cinerea* encodes two DCL proteins. The *dcl1 dcl2* double mutant exhibited significantly reduced virulence in both Arabidopsis and tomato (*Solanum lycopersicum*) (Weiberg *et al.*, 2013). In this study, we found only one RNase III Dicer-like protein in *Pst*. The transcript levels of *PsDCL* showed an increase during wheat–*Pst* interactions. Moreover, the expression of *Pst*-milR1 was inhibited in *PsDCL* knockdown plants. This resulted in a reduction in *Pst* virulence. Thus, we infer that *Pst*-milR1 may be a Dicer-dependent sRNA. *PsDCL* may participate in virulence by producing milRNAs.

In conclusion, *Pst*-milR1 was confirmed and identified from *Pst*. *Pst*-milR1 is induced during wheat–*Pst* interactions. *Pst*-milR1 may function as an effector to inhibit host *PR2* (*SM638*), which probably contributes to wheat resistance to *Pst*. In addition, *PsDCL* may take part in the generation of *Pst*-milR1, but the detailed mechanisms require further exploration.

Author contributions

B.W., Y.S., M.Z., R.L., N.S. and H.F. performed the research; B.W. and X.W. drew figures and drafted the manuscript; Z.K. designed the research. All authors reviewed the manuscript.

References

Bartel DP. 2004. MicroRNAs: genomics, biogenesis, mechanism, and function. *Cell* 116: 281–297.

Bartnicki-Garcia S. 1968. Cell wall chemistry, morphogenesis, and taxonomy of fungi. *Annual Reviews in Microbiology* 22: 87–108.

Bowles DJ. 1990. Defense-related proteins in higher plants. *Annual Review of Biochemistry* 59: 873–907.

Buck AH, Coakley G, Simbari F, McSorley HJ, Quintana JF, Le Bihan T, Kumar S, Abreu-Goodger C, Lear M, Ceroni A. 2014. Exosomes secreted by nematode parasites transfer small RNAs to mammalian cells and modulate innate immunity. *Nature Communications* 5: 5488.

Cheng Y, Wang X, Yao J, Voegele RT, Zhang YR, Wang WM, Huang LL, Kang ZS. 2015. Characterization of protein kinase PsSRPKL, a novel pathogenicity factor in the wheat stripe rust fungus. *Environmental Microbiology* 17: 2601–2617.

Croce CM. 2009. Causes and consequences of microRNA dysregulation in cancer. *Nature Reviews Genetics* 10: 704–714.

Dang Y, Yang Q, Xue Z, Liu Y. 2011. RNA interference in fungi: pathways, functions, and applications. *Eukaryotic Cell* 10: 1148–1155.

Fal K, Landrein B, Hamant O. 2016. Interplay between miRNA regulation and mechanical stress for CUC gene expression at the shoot apical meristem. *Plant Signaling & Behavior* 11: e1127497.

Feng H, Huang X, Zhang Q, Wei G, Wang X, Kang Z. 2012. Selection of suitable inner reference genes for relative quantification expression of microRNA in wheat. *Plant Physiology and Biochemistry* 51: 116–122.

Fudal I, Collemare J, Böhnert HU, Melayah D, Lebrun M-H. 2007. Expression of *Magnaporthe grisea* avirulence gene *ACE1* is connected to the initiation of appressorium-mediated penetration. *Eukaryotic Cell* 6: 546–554.

Fulci V, Macino G. 2007. Quelling: post-transcriptional gene silencing guided by small RNAs in *Neurospora crassa*. *Current Opinion in Microbiology* 10: 199–203.

Ghildiyal M, Zamore PD. 2009. Small silencing RNAs: an expanding universe. *Nature Reviews Genetics* 10: 94–108.

Hein I, Barciszewska-Pacak M, Hrubikova K, Williamson S, Dinesen M, Soenderby IE, Sundar S, Jarmolowski A, Shirasu K, Lacomme C. 2005. Virus-induced gene silencing-based functional characterization of genes associated with powdery mildew resistance in barley. *Plant Physiology* 138: 2155–2164.

Jefferson RA, Kavanagh TA, Bevan MW. 1987. GUS fusions: beta-glucuronidase as a sensitive and versatile gene fusion marker in higher plants. *The EMBO Journal* 6: 3901–3907.

Jones-Rhoades MW, Bartel DP, Bartel B. 2006. MicroRNAs and their regulatory roles in plants. *Annual Review of Plant Biology* 57: 19–53.

Kang K, Zhong J, Jiang L, Liu G, Gou CY, Wu Q, Wang Y, Luo J, Gou D. 2013. Identification of microRNA-Like RNAs in the filamentous fungus *Trichoderma reesei* by solexa sequencing. *PLoS One* 8: e76288.

Kang Z, Huang L, Buchenauer H. 2002. Ultrastructural changes and localization of lignin and callose in compatible and incompatible interactions between wheat and *Puccinia striiformis*. *Journal of Plant Diseases and Protection* 109: 25–37.

Kim VN, Han J, Siomi MC. 2009. Biogenesis of small RNAs in animals. *Nature Reviews Molecular Cell Biology* 10: 126–139.

Knip M, Constantin ME, Thordal-Christensen H. 2014. Trans-kingdom cross-talk: small RNAs on the move. *PLoS Genetics* 10: e1004602.

Koch A, Biedenkopf D, Furch A, Weber L, Rossbach O, Abdellatef E, Linicus L, Johannsmeier J, Jelonek L, Goesmann A et al. 2016. An RNAi-based control of *Fusarium graminearum* infections through spraying of long dsRNAs involves a plant passage and is controlled by the fungal silencing machinery. *PLoS Pathogens* 12: e1005901.

Lau SKP, Chow W-N, Wong AYP, Yeung JMY, Bao J, Zhang N, Lok S, Woo PCY, Yuen KY. 2013. Identification of microRNA-like RNAs in mycelial and yeast phases of the thermal dimorphic fungus *Penicillium marneffei*. *PLoS Neglected Tropical Diseases* 7: e2398.

Lee HC, Li L, Gu W, Xue Z, Crosthwaite SK, Pertsemlidis A, Lewis ZA, Freitag M, Selker EU, Mello CC et al. 2010. Diverse pathways generate microRNA-like RNAs and Dicer-independent small interfering RNAs in fungi. *Molecular Cell* 38: 803–814.

Lee RC, Feinbaum RL, Ambros V. 1993. The *C. elegans* heterochronic gene *lin-4* encodes small RNAs with antisense complementarity to *lin-14*. *Cell* 75: 843–854.

Li RQ, Li YR, Kristiansen K, Wang J. 2008. SOAP: short oligonucleotide alignment program. *Bioinformatics* 24: 713–714.

Li W, Faris J, Muthukrishnan S, Liu D, Chen P, Gill B. 2001. Isolation and characterization of novel cDNA clones of acidic chitinases and β-1,3-glucanases from wheat spikes infected by *Fusarium graminearum*. *Theoretical and Applied Genetics* 102: 353–362.

Li Y, Lu YG, Shi Y, Wu L, Xu Y-J, Huang F, Guo X-Y, Zhang Y, Fan J, Zhao JQ. 2014. Multiple rice microRNAs are involved in immunity against the blast fungus *Magnaporthe oryzae*. *Plant Physiology* 164: 1077–1092.

Link T, Seibel C, Voegele RT. 2014. Early insights into the genome sequence of *Uromyces fabae*. *Frontiers in Plant Science* 5: 587.

Liu B, Xue X, Cui S, Zhang X, Han Q, Zhu L, Liang X, Wang X, Huang L, Chen X. 2010. Cloning and characterization of a wheat β-1,3-glucanase gene induced by the stripe rust pathogen *Puccinia striiformis* f. sp. *tritici*. *Molecular Biology Reports* 37: 1045–1052.

Liu C, Pedersen C, Schultz-Larsen T, Aguilar GB, Madriz-Ordeñana K, Hovmøller MS, Thordal-Christensen H. 2016. The stripe rust fungal effector PEC6 suppresses pattern-triggered immunity in a host species-independent manner and interacts with adenosine kinases. *New Phytologist* 213: 1556.

Liu N, Tu L, Wang L, Hu H, Xu J, Zhang X. 2017. MicroRNA 157-targeted SPL genes regulate floral organ size and ovule production in cotton. *BMC Plant Biology* 17: 7.

Liu N, Wu S, Van Houten J, Wang Y, Ding B, Fei ZJ, Clarke TH, Reed JW, Van Der Knaap E. 2014. Down-regulation of AUXIN RESPONSE FACTORS 6 and 8 by microRNA 167 leads to floral development defects and female sterility in tomato. *Journal of Experimental Botany* 65: 2507–2520.

Livak KJ, Schmittgen TD. 2001. Analysis of relative gene expression data using real-time quantitative PCR and the $2^{-\Delta\Delta CT}$ method. *Methods* 25: 402–408.

Lo Presti L, Lanver D, Schweizer G, Tanaka S, Liang L, Tollot M, Zuccaro A, Reissmann S, Kahmann R. 2015. Fungal effectors and plant susceptibility. *Annual Review of Plant Biology* 66: 513–545.

Long XR, He Y, Huang C, Li J. 2014. MicroRNA-148a is silenced by hypermethylation and interacts with DNA methyltransferase 1 in hepatocellular carcinogenesis. *International Journal of Oncology* 44: 1915–1922.

Luo H, Wang X, Zhan G, Wei G, Zhou X, Zhao J, Huang L, Kang Z. 2015. Genome-wide analysis of simple sequence repeats and efficient development of polymorphic SSR markers based on whole genome re-sequencing of multiple isolates of the wheat stripe rust fungus. *PLoS ONE* 10: e0130362.

Mauch F, Staehelin LA. 1989. Functional implications of the subcellular localization of ethylene-induced chitinase and beta-1, 3-glucanase in bean leaves. *The Plant Cell* 1: 447–457.

Merelo P, Ram H, Caggiano MP, Ohno C, Ott F, Straub D, Graeff M, Cho SK, Yang SW, Wenkel S et al. 2016. Regulation of MIR165/166 by class II and class III homeodomain leucine zipper proteins establishes leaf polarity. *Proceedings of the National Academy of Sciences, USA* 113: 11973–11978.

Meyers BC, Axtell MJ, Bartel B, Bartel DP, Baulcombe D, Bowman JL, Cao X, Carrington JC, Chen X, Green PJ et al. 2008. Criteria for annotation of plant microRNAs. *The Plant Cell* 20: 3186–3190.

Mueth NA, Ramachandran SR, Hulbert SH. 2015. Small RNAs from the wheat stripe rust fungus (*Puccinia striiformis* f. sp. *tritici*). *BMC Genomics* 16: 1.

Murray M, Thompson WF. 1980. Rapid isolation of high molecular weight plant DNA. *Nucleic Acids Research* 8: 4321–4326.

Muthukrishnan S, Liang GH, Trick HN, Gill BS. 2001. Pathogenesis-related proteins and their genes in cereals. *Plant Cell, Tissue and Organ Culture* 64: 93–114.

Navarro L, Dunoyer P, Jay F, Arnold B, Dharmasiri N, Estelle M, Voinnet O, Jones JD. 2006. A plant miRNA contributes to antibacterial resistance by repressing auxin signaling. *Science* 312: 436–439.

Nowara D, Gay A, Lacomme C, Shaw J, Ridout C, Douchkov D, Hensel G, Kumlehn J, Schweizer P. 2010. HIGS: host-induced gene silencing in the obligate biotrophic fungal pathogen *Blumeria graminis*. *The Plant Cell* 22: 3130–3141.

Nunes CC, Gowda M, Sailsbery J, Xue M, Chen F, Brown DE, Oh Y, Mitchell TK, Dean RA. 2011. Diverse and tissue-enriched small RNAs in the plant pathogenic fungus, *Magnaporthe oryzae*. *BMC Genomics* 12: 288.

Panwar V, McCallum B, Bakkeren G. 2013a. Endogenous silencing of *Puccinia triticina* pathogenicity genes through *in planta*-expressed sequences leads to the suppression of rust diseases on wheat. *Plant Journal* 73: 521–532.

Panwar V, McCallum B, Bakkeren G. 2013b. Host-induced gene silencing of wheat leaf rust fungus *Puccinia triticina* pathogenicity genes mediated by the Barley stripe mosaic virus. *Plant Molecular Biology* 81: 595–608.

Petty ITD, Jackson AO. 1990. Mutational analysis of barley stripe mosaic virus RNA β. *Virology* 179: 712–718.

Qutob D, Chapman BP, Gijzen M. 2013. Transgenerational gene silencing causes gain of virulence in a plant pathogen. *Nature Communications* 4: 1349.

Raman V, Simon SA, Romag A, Demirci F, Mathioni SM, Zhai J, Meyers BC, Donofrio NM. 2013. Physiological stressors and invasive plant infections alter the small RNA transcriptome of the rice blast fungus, *Magnaporthe oryzae*. *BMC Genomics* 14: 326.

Schwessinger B. 2016. Fundamental wheat stripe rust research in the 21st century. *New Phytologist* 213: 1625–1631.

Sela-Buurlage MB, Ponstein AS, Bres-Vloemans SA, Melchers LS, van den Elzen PJ, Cornelissen BJ. 1993. Only specific tobacco (*Nicotiana tabacum*) chitinases and beta-1,3-glucanases exhibit antifungal activity. *Plant Physiology* 101: 857–863.

Sunkar R, Zhu J-K. 2004. Novel and stress-regulated microRNAs and other small RNAs from Arabidopsis. *The Plant Cell* 16: 2001–2019.

Wang B, Sun YF, Song N, Wei JP, Wang XJ, Feng H, Kang ZS. 2014. MicroRNAs involving in cold, wounding and salt stresses in *Triticum aestivum* L. *Plant Physiology and Biochemistry* 80: 90–96.

Wang CF, Huang LL, Buchenauer H, Han QM, Zhang HC, Kang ZS. 2007. Histochemical studies on the accumulation of reactive oxygen species (O^{2-} and H_2O_2) in the incompatible and compatible interaction of wheat–*Puccinia striiformis* f. sp. *tritici*. *Physiological and Molecular Plant Pathology* 71: 230–239.

Wang M, Weiberg A, Lin FM, Thomma BP, Huang HD, Jin H. 2016. Bidirectional cross-kingdom RNAi and fungal uptake of external RNAs confer plant protection. *Nature Plants* 2: 16151.

Wang Q, Han C, Ferreira AO, Yu X, Ye W, Tripathy S, Kale SD, Gu B, Sheng Y, Sui Y. 2011. Transcriptional programming and functional interactions within the *Phytophthora sojae* RXLR effector repertoire. *The Plant Cell* 23: 2064–2086.

Wang YN, Li K, Chen L, Zou Y, Liu H, Tian YP, Li DX, Wang R, Zhao F, Ferguson BJ et al. 2015. microRNA167-directed regulation of the auxin response factors, GmARF8a and GmARF8b, is required for soybean (*Glycine max* L.) nodulation and lateral root development. *Plant Physiology* 168: 984–999.

Weiberg A, Jin H. 2015. Small RNAs – the secret agents in the plant–pathogen interactions. *Current Opinion in Plant Biology* 26: 87–94.

Weiberg A, Wang M, Bellinger M, Jin H. 2014. Small RNAs: a new paradigm in plant-microbe interactions. *Annual Review of Phytopathology* 52: 495–516.

Weiberg A, Wang M, Lin FM, Zhao H, Zhang Z, Kaloshian I, Huang HD, Jin H. 2013. Fungal small RNAs suppress plant immunity by hijacking host RNA interference pathways. *Science* 342: 118–123.

Xiao C, Rajewsky K. 2009. MicroRNA control in the immune system: basic principles. *Cell* 136: 26–36.

Xin M, Wang Y, Yao Y, Xie C, Peng H, Ni Z, Sun Q. 2010. Diverse set of microRNAs are responsive to powdery mildew infection and heat stress in wheat (*Triticum aestivum* L.). *BMC Plant Biology* 10: 123.

Yao Y, Guo G, Ni Z, Sunkar R, Du J, Zhu JK, Sun Q. 2007. Cloning and characterization of microRNAs from wheat (*Triticum aestivum* L.). *Genome Biology* 8: R96.

Yin C, Downey SI, Klages-Mundt NL, Ramachandran S, Chen X, Szabo LJ, Pumphrey M, Hulbert SH. 2015. Identification of promising host-induced silencing targets among genes preferentially transcribed in haustoria of *Puccinia*. *BMC Genomics* 16: 1.

Zhang T, Zhao YL, Zhao JH, Wang S, Jin Y, Chen ZQ, Fang YY, Hua CL, Ding SW, Guo HS. 2016. Cotton plants export microRNAs to inhibit virulence gene expression in a fungal pathogen. *Nature Plants* 2: 16153.

Zhang YC, Liao JY, Li ZY, Yu Y, Zhang JP, Li QF, Qu LH, Shu WS, Chen YQ. 2014. Genome-wide screening and functional analysis identify a large number of long noncoding RNAs involved in the sexual reproduction of rice. *Genome Biology* 15: 512.

Zheng W, Huang L, Huang J, Wang X, Chen X, Zhao J, Guo J, Zhuang H, Qiu CZ, Liu J et al. 2013. High genome heterozygosity and endemic genetic recombination in the wheat stripe rust fungus. *Nature Communications* 4: 2673.

Zhou J, Fu Y, Xie J, Li B, Jiang D, Li G, Cheng J. 2012a. Identification of microRNA-like RNAs in a plant pathogenic fungus *Sclerotinia sclerotiorum* by high-throughput sequencing. *Molecular Genetics and Genomics* 287: 275–282.

Zhou Q, Wang Z, Zhang J, Meng H, Huang B. 2012b. Genome-wide identification and profiling of microRNA-like RNAs from *Metarhizium anisopliae* during development. *Fungal Biology* 116: 1156–1162.

Supporting Information

Additional Supporting Information may be found online in the Supporting Information tab for this article:

Fig. S1 Stem-loop structure of the *Pst*-milR1 precursor. The solid line indicates mature *Pst*-milR1 RNA.

Fig. S2 Alignment of *SM638* with other *PR2* gene sequences from wheat.

Fig. S3 Analysis of the silencing efficiency of *PDS*.

Fig. S4 Transcript profiles of *PR2* genes in *Pst*-milR1 knocked down leaves inoculated with *Pst* race CYR31.

Fig. S5 Transcript profiles of *PR2* genes in *SM638* knocked-down leaves compared with BSMV-γ leaves inoculated with *Pst* races CYR23 and CYR31, respectively.

Fig. S6 Phenotypic changes on wheat leaves of *PsDCL* knocked-down plants.

Table S1 RT-qPCR primers of miRNAs and DNA oligonucleotides

Table S2 Primers for plasmid constructions

Table S3 Prediction of *Pst*-milR1 targets in wheat

Table S4 Results of small RNA sequencing

Table S5 Relative transcription levels of *Pst*-milR1 in *Pst*-milR1 knocked-down leaves challenged with CYR31

Table S6 Histological analysis of *SM638* knocked-down leaves of Su11 responding to CYR31

Please note: Wiley Blackwell are not responsible for the content or functionality of any Supporting Information supplied by the authors. Any queries (other than missing material) should be directed to the *New Phytologist* Central Office.